IEEE Access
Multidisciplinary | Rapid Review | Open Access Journal

Received March 5, 2019, accepted April 23, 2019, date of publication April 29, 2019, date of current version May 7, 2019.

Digital Object Identifier 10.1109/ACCESS.2019.2913553

Identification of the Thermal Parameters for the NH gG Fuse Using the Differential Evolution

MIRZA SARAJLIĆ, (Graduate Student Member, IEEE), MITJA HRIBERNIK, PETER KITAK, (Member, IEEE), AND JOŽE PIHLER, (Member, IEEE)
Faculty of Electrical Engineering and Computer Science, University of Maribor, 2000 Maribor, Slovenia
Corresponding author: Mirza Sarajlić (mirza.sarajlic@um.si)

ABSTRACT This paper describes the identification of the thermal parameters for the high breaking capacity low-voltage NH gG fuse. For the process of parameter's determination, a 3D numerical model of the fuse is used together with the measured temperature on the fuse and differential evolution (DE) as the powerful optimizer for optimization problems. DE's main task is to reduce the difference between the measured and calculated fuse temperatures. The classic DE algorithm is compared with three improved DE algorithms that have a reduction of the population size during the optimization process. The results of all four algorithms are compared, and the most favorable choice of algorithm is given for such temperature coefficient calculations. The fuse model is appropriate for the calculation of the fusing temperature, according to the excellent agreement between the measured and calculated fuse temperatures.

INDEX TERMS Fuse link, temperature, identification, 3D model, differential evolution.

I. INTRODUCTION

Usage of the fuse as a protection element in a power grid started at the beginning of electrification [1], [2]. The fuse is a crucial protection element in all electrical engineering applications. It is a device that opens the electric circuit in which it is installed by melting one or more specially designed and compliant melting elements. The circuit opens when the current value is exceeded at the appropriate time [1]. In cases of serious faults in installations or power networks, the fuse is the vital and last protection barrier. In comparison with other protection devices (i.e. disconnectors, circuit-breakers), the fuse enables the highest breaking capacity in a very short time period (within a few milliseconds), as well as the ability to prevent a short-circuit. This is supported by the simultaneous workings of individual construction parts, mainly a melting element and quartz sand, which has the highest specific heat regarding vaporization. The main task of the fuse is to protect electrical devices, installations and people.

The operating principle of a fuse is simple. Copper wire or a suitably shaped strip (fuse element), which is capable of conducting an electric current under normal conditions, burns out when the current exceeds a certain threshold value. In this case, it is important that the fuse interrupts the smallest part of the power grid. Once the excessive current flows through the fuse, the fuse element overheats and melts. At this point, an electric arc is generated, which evaporates the metal. The electric arc is then distributed into quartz sand, where it is cooled down onto granules. Thus, the quantity of quartz sand granules decreases. In this way, the path of the arc becomes longer, and the intense cooling takes place over the whole path.

The article deals with the NH2 gG 400 A/500 V single phase fuse, used for protection in Low Voltage (LV) networks with a voltage up to 500 V, and is ranked as a fuse for general application (gG) with blade contacts (NH – Niederspannungs Hochleitungs, which is German for low-voltage high-breaking-capacity [2]). NH gG fuse links are used widely in electrical power grids to protect electrical devices in case of overload or short circuit currents [3]. The fuse elements are fixed between two blade contacts in a ceramic body (Fig. 1). In our case, there are four fuse elements. Three fuse elements are the same width, and the fourth fuse element is narrower.

Over the years, different methods [3]–[16] have been used for thermal investigation of fuse links. In [3], the authors investigate the long term behavior of fuse elements at higher thermal stress level. The role of LV/NH fuse links' rated voltage in distribution network losses was examined in [4], where fuses use rated voltage 500 – 690 V AC instead of 400 V AC. In [5]–[11], the authors use 2D and 3D FEM

The associate editor coordinating the review of this manuscript and approving it for publication was Mahammad Abdul Hannan.

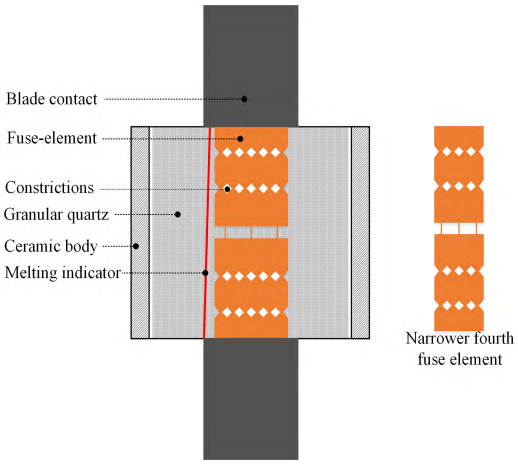

FIGURE 1. Assembly of a NH fuse.

software in order to examine a fuse link's thermal field. In [5], the authors analyze a fuse's thermal field using 3D FEM software, calculating the temperatures inside or on the fuse. A 2D thermal model of a fuse was developed in [6] in order to study the temperature distribution at a fuse. The effect of the current harmonics on the fuse thermal is investigated, and the temperature distribution through all fuse link elements is shown. A 3D FEM software was used in [7] to analyze the transient temperature rise of the fuse elements in current-limiting fuses. The thermal behavior of the fuse link during steady-state conditions was analyzed in [8], when different types of notches are applied using 3D FEM software. In [9], an FE model of a fuse was used to analyze the influence of harmonic content and harmonic frequency by thermoelectric coupling simulation. In [10], an FEM model of a medium voltage fuse was used for thermal analysis. In [11], a 3D model of the Joule heating of the fuse element was developed using a set of equations coupling the thermal and the electrical phenomena, including solid-liquid-vapor phase transitions, in order to evaluate the pre-arcing time in HBC fuses. In [12]–[14] the authors use a mathematical model in order to examine the thermal behavior of a fuse. A mathematical methodology for the calculation of the steady state thermal behavior of a medium voltage fuse was used in [12]. A mathematical model of medium and low voltage fuses was developed in [13], in order to estimate the temperature across the fuse during the pre-arcing period. A mathematical model for the analysis of the steady state thermal behavior of a medium voltage vertically fixed fuse was developed in [14].

A. RESEARCH OBJECTIVES

The main novelty of this paper is a method to identify fuse's thermal parameters using the Differential Evolution (DE) algorithm, fuse temperature calculation using a 3D model, and measured data. These parameters are of crucial importance for the designing process of a fuse, especially for fuses and electrical devices, that use identical materials, like ceramics and granular quartz. Particle Swarm Optimization (PSO) [17], Genetic Algorithm [18], or other, could be used in the optimization process. This paper used the DE, a stochastic optimization algorithm, which is suitable for solving of nonlinear and constrained real-life optimization problems in Engineering [19]–[25].

The classic DE algorithm is compared to three improved DE algorithms, with changing of the population size during the optimization process. The three improved DE algorithms are: the DE algorithm with half-reducing of the population, the DE algorithm with linear-reducing of the population, and the DE algorithm with faster linear reduction of the population. The results of all four algorithms are compared, and the most favorable choice of algorithm is given for such temperature coefficient calculations.

The entire designing and identifying thermal parameters process of the NH gG fuse links is universal, and applicable for fuse links of all voltage levels. The fuse link model was built in EleFAnT 3D [26]. The selected optimization algorithm DE is described in Section IV, where the minimization of the Objective Function has been carried out. The crucial parameter of the Objective Function will be the measured temperature in the interior and exterior of the fuse. The measurements will be carried out under load test.

This paper is organized as follows. Section II describes the performed measurements and the experimental setup. A fuse model is described in Section III. A method for identifying fuse's thermal parameters is presented in Section IV. The obtained parameters are discussed in Section V with the comparison between the calculated and measured fuse's temperatures. The conclusions are presented in Section VI.

II. EXPERIMENTAL SET-UP AND MEASUREMENTS

The measurements have been carried out in a testing laboratory at the Faculty of Electrical Engineering and Computer Science, University of Maribor. The applied experimental set-up (Fig. 2) consists of the testing line with tested fuse, transformers, power analyzer and connection to the power grid.

The test object was a low voltage fuse NH2 gG 400 A/500 V. A power analyzer Norma D5225M was used to measure the current that flowed through the tested fuse. An autotransformer was used to set the voltage of the transformer, which was in a single-phase short circuit in order to acquire the current ($I = 400$ A) that flowed through the tested fuse. During the measurements, the current that flowed through the tested fuse has been coordinated in order to maintain the constant value of 400 A. The measured resistance of the tested fuse at the surrounding temperature 25.5°C was $R_{\text{fuse}} = 0.154\ \text{m}\Omega$, which means that the voltage drop (U_{fuse}) at the fuse is as follows (1):

$$U_{\text{fuse}} = I \cdot R_{\text{fuse}} = 400\text{A} \cdot 0.154 \cdot 10^{-3}\Omega = 0.062\text{V} \quad (1)$$

Temperature measurements of the fuse were carried out using thermocouples, which were attached to different locations on the fuse (outside and inside the fuse, Fig. 3). There were 14 thermocouples (Pt) and their location is shown in Table 1. The measurement was carried out by heating

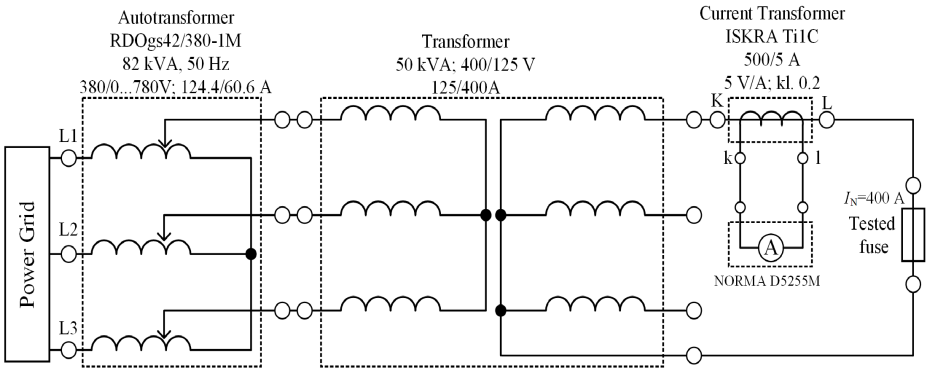

FIGURE 2. Electric scheme of experimental set-up.

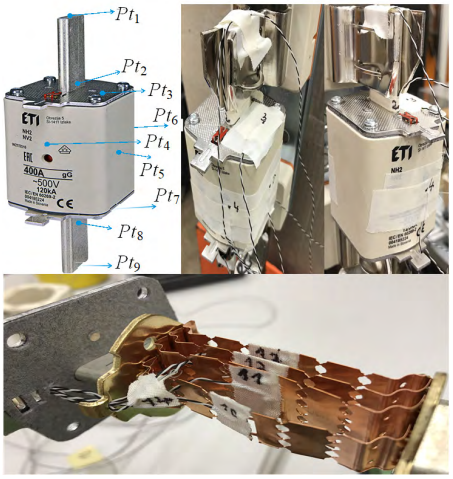

FIGURE 3. Positions of thermocouples on the fuse's outside and inside (fuse links).

TABLE 1. Locations of the thermocouples from Fig. 3.

Thermocouple	Location
Pt_1, Pt_9	On the top part of the upper and lower blade contact, respectively
Pt_2, Pt_8	On the bottom part of the upper and lower blade contact, respectively
Pt_3, Pt_7	On the upper and lower cover of the fuse, respectively
Pt_4, Pt_5, Pt_6	On the ceramic body, namely: The side where the inscription is, the ride side and the rear side of the ceramic body, respectively
Pt_{10}	On the narrower (fourth) fuse element
Pt_{11}, Pt_{12}, Pt_{13}	On the second, third and fourth fuse elements, respectively
Pt_{14}	In the quartz sand inside the fuse

the fuse (joule heating under the current 400 A) until the temperature reached the thermal equilibrium in all parts of the fuse, that is to say, when temperatures are stable within2 K per hour. A thermocouple was bonded at a non-constricted area of the fuse-element with a tape which is suitable for high temperatures. The flow of these temperatures is shown in Fig. 4. The final values of these temperatures (shown in Table 2) are used as the input data for the identification of the fuse's thermal parameters.

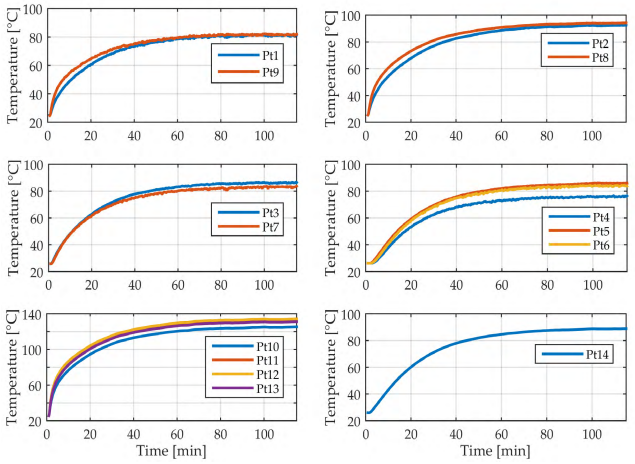

FIGURE 4. Fuse's temperatures between the temperature rise at the current 400 A.

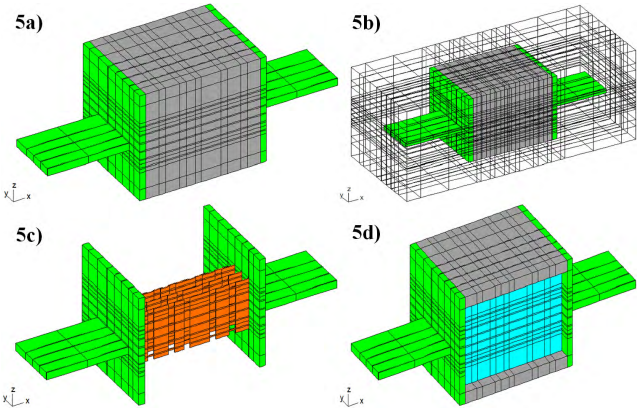

FIGURE 5. a) Fuse model (grey color – ceramic body, green color – blade contacts). b) Finite elements in the whole area of the model. c) Fuse model without ceramic body with visible fuse links (orange color). d) Fuse model without one of the ceramic sides, where the blue color shows granular quartz.

III. FUSE MODEL

The fuse link model is presented in Figs. 5a–5d. Fuse parts are categorized with the colors specified in Table 3, which

TABLE 2. Final values of measured temperatures from Fig. 4.

Thermocouple	Temperature [°C]	Thermocouple	Temperature [°C]
Pt_1	81.32	Pt_8	94.2
Pt_2	92.49	Pt_9	81.91
Pt_3	86.48	Pt_{10}	125.3
Pt_4	76.49	Pt_{11}	134.1
Pt_5	85.95	Pt_{12}	134.4
Pt_6	83.68	Pt_{13}	131.2
Pt_7	83.65	Pt_{14}	88.85

also shows the materials, electric and thermal parameters of each of the components. Finite Elements (FE) (Fig. 5b). The FE analysis is conducted with programme tool EleFAnT 3D [26]. The problem is divided into single geometric shapes that belong to corresponding types of material (Table 3). There are five geometric shapes: Blade contacts (upper and lower contact), ceramic body (four sides), fuse elements (four elements), granular quartz and surrounding area (air). The function of upper and lower contact is to connect the fuse with the circuit in order to protect it [15].

The fuse model is designed as a weak coupled problem that uses electric and thermal models. Calculations of current density J [A/m^2] and electric conductivity σ [S/m] are conducted in the electric model, which serve as the input data (Fig 6, path of the blue arrow) for the calculation of power losses p [W/m^3]. The values of power losses p are then used as input data for the thermal model when calculating the fuse's temperature T (Fig. 6, path of the red arrow). The other input data for calculation of the temperature are thermal conductivity and convection, which are catalogue values given in Table 3. Conduction is the transfer of heat in solid materials with direct contact, and convection is the transfer of heat to the surrounding space [31].

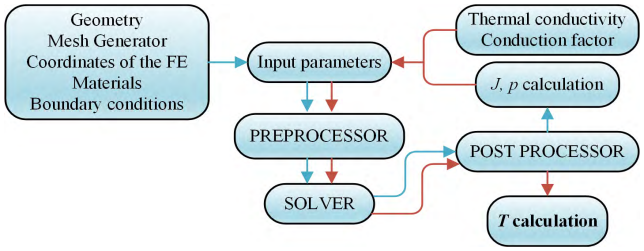

FIGURE 6. Graphic demonstration of process for calculation of the fuse's temperature.

The numerical analysis of temperature calculation for the fuse model has been conducted with the catalogue parameter values from Table 3. For the modeling and simulation, the surrounding area was defined as air with temperature as measured in the laboratory (25.5° C). In order to achieve a fuse's nominal current (400 A), the voltage drop on the fuse is defined as 0.072 V. It can be seen that the value of voltage drop used for simulation (0.072 V) and measured one (0.062 V) is almost the same. The measured voltage drop is 0.062 V and it represents the basis for the numerical calculations. Regarding the simplifications in the numerical model, the value of the voltage drop (0.072 V) is adapted to the numerical model in order to achieve the current of 400 A. The measured and calculated values of the fuse temperatures are compared. The obtained results are shown in Table 4.

The results presented in Table 4 show the deviations between measured and calculated temperature, that are between 7.39° C and 34.44° C. This could be considered as inadequate and requiring improvement. Hence, the main idea of this paper is reducing the deviation between measured and calculated fuse temperature with the purpose of improving the accuracy of the numerical fuse model. This is done in the suggested DE based optimization procedure, where the measured data and fuse model are used together in order to determine those values of parameters for thermal conductivity and convection factor.

IV. IDENTIFICATION OF THE FUSE THERMAL PARAMETERS USING DE

The engineering audience [19], [21], [24], [31] uses DE, as it is a fast and robust stochastic optimization algorithm. It was first introduced by Storn and Price [20]. This algorithm is appropriate for solving nonlinear and constrained optimization problems [24]. It has been selected as an suitable optimization algorithm, because of its simple application and effectiveness. Detailed descriptions of the DE algorithm are available in [20] and [25]. Table 5 presents the used DE settings.

DE determines the thermal parameters p_i, where $i = [1, 2, \ldots, 7]$. These parameters are: Thermal conductivity of blade contact (p_1), ceramic body (p_2), fuse element (p_3), granular quartz (p_4) and surrounding area (air, p_5); convection factor of blade contacts (p_6) and ceramic body (p_7). During the optimization process, the DE is minimising the value of the Objective Function z (2):

$$z = \sum_{\mathrm{i}=1}^{7} z_\mathrm{i} \tag{2}$$

where z_i are partial Objective Functions, that are written as:

$$z_\mathrm{i} = \begin{cases} \sqrt{\sum_{\mathrm{j}} \left(Pt_{\mathrm{jmeas}} - Pt_{\mathrm{jcalc}}\right)^2} \\ \quad \text{if } j \in \{[10]\,;\,[14]\} \\ \frac{1}{2}\sqrt{\sum_{\mathrm{j}} \left(Pt_{\mathrm{jmeas}} - Pt_{\mathrm{jcalc}}\right)^2} \\ \quad \text{if } j \in \{[1,9]\,;\,[2,8]\,;\,[3,7]\} \\ \frac{1}{3}\sqrt{\sum_{\mathrm{j}} \left(Pt_{\mathrm{jmeas}} - Pt_{\mathrm{jcalc}}\right)^2} \\ \quad \text{if } j \in \{[4,5,6]\,;\,[11,12,13]\} \end{cases}$$
$$i = [1, 2, \ldots, 7] \tag{3}$$

There are seven partial Objective Functions z_i, hence $i = [1, 2, \ldots, 7]$. j presents thermocouples, which were attached to different locations on the fuse (outside and inside the fuse). Weights 1, 1/2 and 1/3 in (3) were chosen based on the number of thermocouples within the sum. Objective

TABLE 3. Description of geometric shapes from Fig. 5 [15], [16], [27]–[30].

Colour	Geometric shape	Material	Electric conductivity [S/m]	Thermal conductivity [W/m·K]	Convection factor [W/m²·K]
Green	Blade contact	Metal	$11 \cdot 10^6$	237	8
Grey	Ceramic body	Ceramics	$1 \cdot 10^{-9}$	2.5	7.5
Orange	Fuse elements	Metal	$57 \cdot 10^6$	401	
Blue	Granular quartz	Quartz sand	$1 \cdot 10^{-9}$	1	
White (no colour)	Surrounding area	Air	$1 \cdot 10^{-9}$	0.0257	

TABLE 4. Measured (T_{meas}) and calculated (T_{calc}) temperatures of the fuse.

Measuring point	T_{meas} [°C]	T_{calc} [°C]	$\lvert T_{meas} - T_{calc} \rvert$ [°C]
Pt_1	81.32	108.43	27.11
Pt_2	92.49	109.18	16.69
Pt_3	86.48	110.23	23.75
Pt_4	76.49	109.51	33.02
Pt_5	85.95	120.39	34.44
Pt_6	83.68	109.19	25.51
Pt_7	83.65	109.93	26.28
Pt_8	94.2	108.91	14.71
Pt_9	81.91	108.14	26.23
Pt_{10}	125.3	117.09	8.21
Pt_{11}	134.1	123.81	10.29
Pt_{12}	134.4	124.11	10.29
Pt_{13}	131.2	123.81	7.39
Pt_{14}	88.85	118.02	29.17

TABLE 5. DE settings.

Parameter	Value
Number of parameters D	7
Population size NP	40
Weighting factor F	0.5
Crossover constant CR	0.7
Maximum number of iterations $iter_{max}$	250

Function (2) evaluates the quality of the parameter values applied in the fuse model. Fig. 7 presents the procedure for determining the fuse model's parameters.

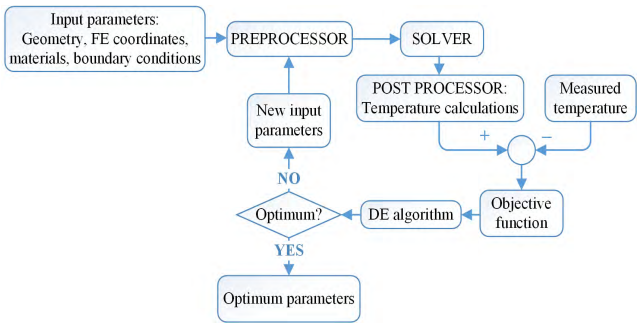

FIGURE 7. Graphic demonstration of procedure for determining the fuse's thermal parameters.

Table 6 presents the boundaries (minimum and maximum values) of optimization variables during the optimization process. These values are selected based on the Ref. [15], [16], [27]–[30].

TABLE 6. Minimum and maximum values of optimization variables.

Parameter	Minimum value	Maximum value
p_1 [W/m·K]	0.0244	0.0270
p_2 [W/m·K]	225.15	248.85
p_3 [W/m·K]	0.8	2.0
p_4 [W/m·K]	0.5	7.5
p_5 [W/m·K]	380.95	441.10
p_6 [W/m²·K]	1	20
p_7 [W/m²·K]	1	15

A. MODIFICATION OF THE DE ALGORITHM: REDUCTION OF HALF OF THE POPULATION

Population size NP is the significant parameter of the DE, which is constant in the classic DE algorithm. The population size can be decreased by gradual reduction, as it is proposed in [32], where it is reduced by half within each block of the block of the predefined generation number. At the beginning of the optimization process, a greater number of individuals is needed, due to the diversity of the population. During the optimization process, the population reduces gradually, and it is the smallest at the end of the process. The population size reduction step is defined as:

$$x_{i,G} = \begin{cases} x_{\frac{NP}{2}+i,G}; & \text{if } f(x_{\frac{NP}{2}+i,G}) < f(x_{i,G}) \\ & \text{and } G = G_R, \\ x_{i,G}; & \text{otherwise.} \end{cases} \quad (4)$$

The new population size is then calculated as:

$$NP_{G+1} = \begin{cases} \frac{NP_{G+1}}{2} & \text{if } G = G_R, \\ NP_G & \text{otherwise.} \end{cases} \quad (5)$$

The generation whose population is going to be reduced is indicated with G_R.

In this paper, the reduction of the population is performed as follows: In the first 5 iterations the algorithm executes calculations using the whole population (pop_{NP}). The algorithm sorts the individuals with regard to the Objective Function from the best to the worst. A new sorted population goes to the next iteration. In the 6th iteration, the algorithm takes half of the population and calculates with the reduced population ($pop_{NP1/2}$) by the same principle. In the 21th iteration, the algorithm takes half of the $pop_{NP1/2}$, and performs calculations with the new population $pop_{NP1/4}$. In the 41th iteration, the algorithm takes half of the $pop_{NP1/4}$ and performs

calculations to the end of the optimization process with the new population $pop_{NP1/8}$.

That means, if the initial population size is $NP = NP_{initial} = 40$:

- After the 5th iteration $NP = NP_{initial}/2 = 20$;
- After the 20th iteration $NP = NP_{initial}/4 = 10$ and
- After the 40th iteration $NP = NP_{initial}/8 = 5$.

B. MODIFICATION OF THE DE ALGORITHM: LINEAR REDUCTION OF THE POPULATION

This algorithm is based on the linear reduction of the population, which is calculated as:

$$NP = NP_{\max} - \frac{NP_{\max} - NP_{\min}}{iter_{\max}} \cdot iter \tag{6}$$

where NP_{max} is the maximum population size; NP_{min} is the minimum population size; $iter_{max}$ is the maximum number of iterations; $iter$ is the current iteration. The user defines NP_{max}, NP_{min} and $iter_{max}$.

In this paper, $NP_{max} = 40$ and $NP_{min} = 10$ is chosen, so the linear reduction could be carried out from 40 to 10 individuals. Likewise, with the algorithm described in subsection IV.A., in this algorithm, the individuals are sorted from the best to the worst with respect to the Objective Function.

C. MODIFICATION OF THE DE ALGORITHM: FASTER LINEAR REDUCTION OF THE POPULATION

This algorithm is an improved version of the algorithm described in subsection IV.B. An improvement is made in terms of faster calculation, i.e. faster reduction of the population. Firstly, the linear NP_{lin} is calculated (7):

$$NP_{\text{lin}} = NP_{\max} - \frac{NP_{\max} - NP_{\min}}{iter_{\max}} \cdot iter \tag{7}$$

and then the new NP(8) is calculated:

$$NP_{\text{new}} = NP_{\text{lin}} - AddRed \tag{8}$$

where $AddRed$ is an additional reduction that is defined as the difference (9) between the Objective Function value from the previous and current iterations:

$$AddRed = round\,|bestval_{iter-1} - bestval_{iter}| \tag{9}$$

where $bestval_{iter-1}$ is the Objective Function value from the previous iteration, and $bestval_{iter}$ is the Objective Function value from the current iteration.

NP_{new} is then used for the calculation of remaining members of the population (NP_{rem}), which is calculated as the difference between NP_{new} and NP_{perc} (10):

$$NP_{\text{rem}} = NP_{\text{new}} - NP_{\text{perc}} \tag{10}$$

NP_{perc} presents the first 20-40% members of the entire population. This percentage is defined by the user at the start of the optimization process.

TABLE 7. Determined fuse model parameters in the suggested optimization process.

Parameter	Value after Optimization				Value before Optimization
	Classical DE	RHP	LRP	FLRP	
p_1 [W/m·K]	0.025	0.0257	0.0254	0.025	0.0257
p_2 [W/m·K]	225.15	225.15	239.06	226	237
p_3 [W/m·K]	0.96	0.96	0.96	0.97	1
p_4 [W/m·K]	7.5	7.5	7.5	7.5	2.5
p_5 [W/m·K]	441	439	432	441	401
p_6 [W/m²·K]	12	12	12	12	8
p_7 [W/m²·K]	12	12.1	12.05	11.95	7.5

TABLE 8. Results after the optimization.

Algorithm	*bestval*	*nfeval*	CPU time [seconds]
Classical DE	0.2210	10001	294360
RHP	0.2214	1716	52440
LRP	0.2225	4163	121680
FLRP	0.2219	2916	86160

In the next step, a matrix is formed, made from zeros and ones:

$$nn = |NP_{\text{rem}} - |NP_{\text{new}} - NP_{\text{lin}}|| \tag{11}$$

where nn is the number of ones in the aforementioned matrix. The ones are arranged at random positions in the matrix. The algorithm compares the matrix made from zeros and ones with the matrix of Objective Function values for every member of the population, with regard to the position of the ones. The positions of ones from the matrix of zeros and ones are taken, and the members of the population with the same position go into the new matrix. This new matrix is smaller than the previous matrix, and the population size of the new matrix is the new value of NP for the next iteration. Fig. 8 summarizes this process briefly.

In this way, this algorithm has a double reduction of the population, which makes it faster than the previous algorithms described in subsections IV.A. and IV.B.

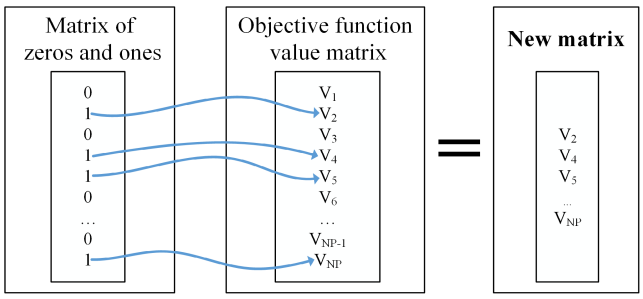

FIGURE 8. Representation of the new matrix formation.

V. RESULTS

The suggested method for determining a fuse's thermal parameters is confirmed comparing the measured and calculated results. The measured temperatures were used in the suggested optimization procedure in order to identify the fuse's thermal parameters. The obtained parameters values

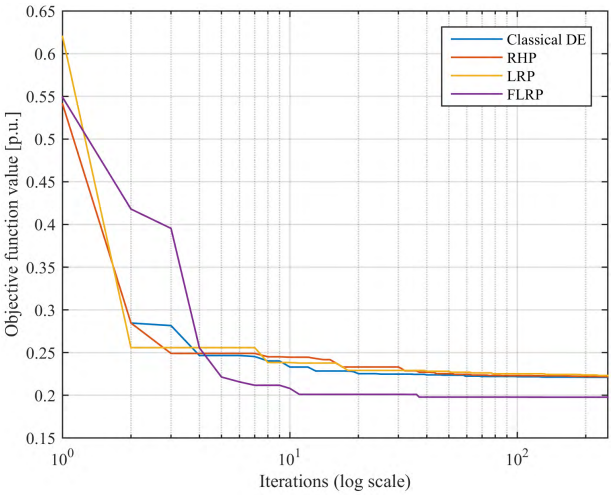

FIGURE 9. Objective function values throughout the generations.

are shown in Table 7, where RHP stands for the Reduction of Half of the Population, LRP stands for the Linear Reduction of the Population and FLRP stands for the Faster Linear Reduction of the Population. From the obtained results in Table 7, it can be seen that all four algorithms gave almost the same values of determined parameters with insignificant deviation of 1 %.

Table 8 shows the mean values of Objective Function (*bestval*), number of Objective Function evaluations (*nfeval*), and CPU time of the calculation. All four algorithms have the same Objective Function value (0.22), with insignificant deviation of the last two decimals. Modified algorithms have less Objective Function evaluations than the Classical DE. The RHP algorithm has the smallest number of Objective Function evaluations (1716), which is almost 6 times smaller than Classical DE's number of Objective Function evaluations. The LRP and FLRP algorithms have almost 2.5 and 3.5, respectively, a lower number of Objective Function evaluations than the Classical DE. As far as the CPU time of the optimization process duration is concerned, the RHP and FLRP algorithms use less time and are 5.6 and 3.4 times faster than the Classical DE, respectively. An example of the Objective Function values' convergence obtained with the Classical and modified DE algorithms is shown in Fig. 9. It can be seen that the FLRP algorithm converges faster in later iterations.

The identified fuse model parameters, shown in Table 7, were used in all following calculations. The measured and calculated temperature using the catalogue and identified parameters are compared in Table 9. The results presented in Table 9 show very good agreement between measured and calculated results using identified parameters, where the average difference is smaller than 3°C and the highest difference is 10°C, which is acceptable.

The following case is used to check the performance of the suggested parameter determination method and corresponding fuse model. In the given case the fuse has two fuse elements, which are the same width, and the current that flows through the fuse is 200 A. There are 12 thermocouples with the same location as in Table 1, apart from thermocouples Pt_{10} and Pt_{12}, as these two fuse elements were removed. The determined parameters from Table 7 are applied, together with the measured temperature. The measured and calculated fuse temperatures are compared in Table 10 with very good agreement, where the difference is smaller than 2.5°C and the highest difference is 4°C, which presents an insignificant difference.

TABLE 9. Measured and calculated fuse temperatures using catalogue and identified parameters under the current 400 A.

Measuring Point			Pt_1	Pt_2	Pt_3	Pt_4	Pt_5	Pt_6	Pt_7	Pt_8	Pt_9	Pt_{10}	Pt_{11}	Pt_{12}	Pt_{13}	Pt_{14}
Temperature [°C]	Measured		81.32	92.49	86.48	76.49	85.95	83.68	86.65	94.2	81.91	125.3	134.1	134.4	131.2	88.85
	Model – calculated	Catalogue parameters	108.43	109.18	110.23	109.51	120.39	109.19	109.93	108.91	108.14	117.09	123.81	124.11	123.81	118.02
		Classical DE	80.93	82.06	82.67	83.09	81.98	80.07	82.73	82.26	81.06	121.26	132.47	132.20	129.41	82.50
		RHP	80.73	81.85	82.47	82.88	81.77	79.86	82.53	82.06	80.86	121.08	132.29	132.01	129.22	82.29
		LRP	80.86	81.92	82.50	82.99	81.85	79.97	82.56	82.12	80.99	121.23	132.44	132.16	129.34	82.39
		FLRP	81.02	82.15	82.76	83.22	82.07	80.18	82.82	82.35	81.15	121.31	132.52	132.25	129.48	82.59

TABLE 10. Measured and calculated fuse temperatures using catalogue and identified parameters under the current 200 A (fuse has two fuse elements).

Measuring Point			Pt_1	Pt_2	Pt_3	Pt_4	Pt_5	Pt_6	Pt_7	Pt_8	Pt_9	Pt_{11}	Pt_{13}	Pt_{14}
Temperature [°C]	Measured		47.57	51.74	50.19	47.26	50.47	49.81	47.91	51.81	46.98	75.18	76.46	50.59
	Model – calculated	Catalogue parameters	57.83	58.24	58.83	60.10	63.68	59.98	58.66	58.09	57.67	68.31	68.31	64.66
		Classical DE	48.64	49.24	49.67	51.33	49.42	48.50	49.84	49.43	48.73	73.43	75.38	49.49
		RHP	48.56	49.15	49.58	51.24	49.33	48.41	49.75	49.34	48.65	73.35	75.29	49.39
		LRP	48.62	49.18	49.59	51.29	49.35	48.46	49.76	49.36	48.71	73.43	75.36	49.44
		FLRP	48.68	49.28	49.71	51.39	49.46	48.55	49.88	49.46	48.77	73.43	75.39	49.53

VI. CONCLUSIONS

This paper applies the DE to identify the thermal parameters of low voltage NH gG fuse in order to estimate the fuse's temperature. The parameter's determination process uses the 3D fuse model, measured fuse temperature and DE algorithm.

The main goal of this paper is to find those fuse thermal parameters with the minimal difference between the measured and calculated fuse temperatures. These parameters are of crucial importance for the designing process of a fuse. Also, they are essential during the minimization of financial costs. The obtained parameters can be used for the newly designed high breaking capacity fuses and other similar apparatus that uses the identical materials, like ceramics and quartz sand.

The obtained parameters can afterwards be used in different conditions (different current 200 A, lesser fuse links) of fuse operation, presenting a very good agreement between the measured and calculated fuse temperatures. It is appropriate for different working conditions and for different fuse types. The suggested method together with the fuse model represent an excellent tool for predicting the maximum tolerable temperature of a high breaking capacity low voltage fuse. Aside from the classical DE optimization algorithm, three improved DE algorithms were used, based on the dynamic changing of the population. All of the tested algorithms are appropriate for determination of thermal parameters in applications as described in this article. However, in terms of Objective Function evaluation using the Finite Element Method, which is time consuming, the crucial information is CPU time of optimization process duration. Hence, the most appropriate algorithm among the tested ones are the RHP and FLRP algorithms.

REFERENCES

[1] J. Pihler *et al.*, "Fuse application in medium voltage switchgear," in *Proc. 9th Int. Conf. Electr. Fuses Appl. (ICEFA)*, Maribor, Slovenia, 2011, pp. 110–118.

[2] A. Wright and P. G. Newberry, *Electric Fuses*, 3rd ed. London, U.K.: 2004.

[3] C. Kühnel, S. Schlegel, and S. Großmann, "Investigations on the long-term behavior and switching function of fuse-elements for NH-fuse-links (gG) at higher thermal stress," in *Proc. 6th Int. Youth Conf. Energy (IYCE)*, Budapest, Hungary, Jun. 2017, pp. 1–8.

[4] C. S. Psomopoulos, G. C. Ioannidis, and Y. Karras, "Role of low-voltage/NH fuselinks rated voltage in distribution network losses. An evaluation based on the Hellenic low-voltage distribution network," *IET Gener., Transmiss. Distrib.*, vol. 8, no. 5, pp. 803–810, Feb. 2014.

[5] A. Plesca, "A complete 3D thermal model for fast fuses," in *Proc. 8th Int. Conf. Electr. Fuses Appl.*, Clermont-Ferrand, France, Sep. 2007, pp. 79–85.

[6] H. F. Farahani, M. Asadi, and A. Kazemi, "Analysis of thermal behavior of power system fuse using finite element method," in *Proc. 4th Int. Power Eng. Optim. Conf. (PEOCO)*, Shah Alam, Malaysia, Jun. 2010, pp. 189–195.

[7] Y. Kawase, T. Miyatake, and S. Ito, "Heat analysis of a fuse for semiconductor devices protection using 3-D finite element method," *IEEE Trans. Magn.*, vol. 36, no. 4, pp. 1377–1380, Jul. 2000.

[8] G. Chiriac, "Thermal analysis of fuses with variable cross-section fuselinks," *Electr. Power Syst. Res.*, vol. 92, pp. 73–80, Nov. 2012.

[9] R. Han, T. Wang, Q. Wang, Y. Zheng, and L. Dong, "Analysis for fusing time of fuse under effect of harmonics based on FE method," in *Proc. China Int. Conf. Electr. Distrib. (CICED)*, Xi'an, China, Aug. 2016, pp. 1–5.

[10] E. Torres, E. Fernandez, A. J. Mazon, I. Zamora, and J. C. Perez, "Thermal analysis of medium voltage fuses using the finite element method," in *Proc. IEEE Russia Power Tech*, St. Petersburg, Russia, Jun. 2005, pp. 1–5.

[11] D. Rochette, W. Bussiere, R. Touzani, S. Memiaghe, G. Velleaud, and P. Andre, "Modelling of the pre-arcing period in HBC fuses including solid-liquid-vapour phase changes of the fuse element," in *Proc. 8th Int. Conf. Electr. Fuses Appl.*, Clermont-Ferrand, France, Sep. 2007, pp. 87–93.

[12] E. Torres, A. J. Mazón, E. Fernández, I. Zamora, and J. C. Pérez, "Thermal performance of back-up current-limiting fuses," *Electr. Power Syst. Res.*, vol. 80, no. 12, pp. 1469–1476, Dec. 2010.

[13] C. S. Psomopoulos and C. G. Karagiannopoulos, "Temperature distribution of fuse elements during the pre-arcing period," *Electr. Power Syst. Res.*, vol. 61, no. 3, pp. 161–167, Apr. 2002.

[14] E. Fernandez, E. Torres, I. Zamora, A. J. Mazon, and I. Albizu, "Thermal model for current limiting fuses installed in vertical position," *Electr. Power Syst. Res.*, vol. 107, pp. 167–174, Feb. 2014.

[15] A. Hamler, S. Gril, and J. P. Cukovic, "Thermal analysis and temperature calculation for the NV melting fuse," in *Proc. 9th Int. Conf. Electr. Fuses Their Appl.*, Sep. 2011, pp. 12–14.

[16] A. Plesca, "Temperature distribution of HBC fuses with asymmetric electric current ratios through fuselinks," *Energies*, vol. 11, no. 8, p. 1990, Jul. 2018.

[17] P. Kitak, A. Glotic, and I. Ticar, "Heat transfer coefficients determination of numerical model by using particle swarm optimization," *IEEE Trans. Magn.*, vol. 50, no. 2, pp. 933–936, Feb. 2014.

[18] K. Higashikawa, T. Nakamura, T. Hoshino, and I. Muta, "Design of bi-2223/Ag coil based on genetic algorithm and finite element method," *IEEE Trans. Appl. Supercond.*, vol. 15, no. 2, pp. 1895–1898, Jun. 2005.

[19] M. Sarajlic, M. Pocajt, P. Kitak, N. Sarajlic, and J. Pihler, "Covered overhead conductor temperature coefficient identification using a differential evolution optimization algorithm," *B&H Electr. Eng.*, vol. 11, pp. 26–35, Jan. 2017.

[20] R. Storn and K. Price, "Differential evolution—A simple and efficient heuristic for global optimization over continuous spaces," *J. Global Optim.*, vol. 11, pp. 341–359, Dec. 1997.

[21] M. Sarajlic, P. Kitak, and J. Pihler, "New design of a medium voltage indoor post insulator," *IEEE Trans. Dielectr. Electr. Insul.*, vol. 24, no. 2, pp. 1162–1168, Apr. 2017.

[22] A. Glotic, N. Sarajlic, M. Kasumovic, M. Tesanovic, M. Sarajlic, and J. Pihler, "Identification of thermal parameters for transformer FEM model by differential evolution optimization algorithm," in *Proc. Int. Conf. Multidisciplinary Eng. Design Optim. (MEDO)*, Belgrade, Serbia, Sep. 2016, pp. 1–6.

[23] M. Sarajlic, J. Pihler, N. Sarajlic, and P. Kitak, "Electric field of a medium voltage indoor post insulator," in *Proc. Electr. Field IntechOpen*, Dec. 2018, pp. 145–159.

[24] M. Sarajlic, J. Pihler, N. Sarajlic, and G. Štumberger, "Identification of the heat equation parameters for estimation of a bare overhead conductor's temperature by the differential evolution algorithm," *Energies*, vol. 11, no. 8, p. 2061, 2018.

[25] K. V. Price, R. M. Storn, and J. A. Lampinen, *Differential Evolution—A Practical Approach to Global Optimization*, 1st ed. Springer-Verlag: Berlin Heidelberg, Germany: 2005.

[26] *Program Tools EleFAnT 3D*. Inst. Fundam. Theory Electr. Eng., Graz, Austria, 2000.

[27] R. Holm, *Electric Contacts Theory and Application*, 4th ed. Springer-Verlag Berlin Heidelberg, Germany: GmbH, 1981.

[28] T. M. Tritt, *Thermal Conductivity: Theory, Properties, and Applications*. New York, NY, USA: Kluwer, 2004.

[29] H. A. Radi and J. O. Rasmussen, *Principles of Physics: For Scientists and Engineers*. Berlin, Germany: Springer-Verlag, 2013.

[30] H. Recknagel, E. Sprenger, and E. R. Schramek,*Taschenbusch fÃijr Heizung + Klima Technik 09/10*. Munich, Germany: Oldenbourg Industrieverlag GmbH, 2009.

[31] M. Sarajlic, M. Pocajt, P. Kitak, N. Sarajlic, and J. Pihler, "Bare conductor temperature coefficient identification by means of differential evolution algorithm," in *Proc. Int. Symp. Innov. Interdiscipl. Appl. Adv. Technol.*, Nov. 2018, pp. 316–325.

[32] J. Brest and M. S. Maucec, "Population size reduction for the differential evolution algorithm," *Appl. Intell.*, vol. 29, no. 3, pp. 228–247, 2008.

MIRZA SARAJLIĆ was born in Tuzla, Bosnia and Herzegovina, in 1991. He received the B.Sc. and M.Sc. degrees in electrical engineering from the Faculty of Electrical Engineering and Computer Science, University of Maribor, Slovenia, in 2013 and 2015, respectively. He is currently pursuing the Ph.D. degree in electrical engineering with the Faculty, where he has been a Faculty Member, since 2015. His research interests include modeling and testing switchgear, and optimization models.

MITJA HRIBERNIK was born in Slovenj Gradec, Slovenia, in 1983. He received the B.S. degree in electrical engineering from the Faculty of Electrical Engineering and Computer Science, University of Maribor, Slovenia, in 2010, where he has been a Faculty Member, since 2007. His research interests include electric machines and regulated electromotor drives.

PETER KITAK (M'09) was born in Ptuj, Slovenia, in 1974. He received the B.S. and Ph.D. degrees in electrical engineering from the Faculty of Electrical Engineering and Computer Science, University of Maribor, Slovenia, in 1999 and 2006, respectively, where he has been a Faculty Member, since 2002. His research interests include modeling insulators and switchgears, numerical calculation of electromagnetic fields, and optimization methods.

JOŽE PIHLER (M'90) was born in Ptuj, Slovenia, in 1955. He received the B.S., M.S., and Ph.D. degrees in electrical engineering from the University of Maribor, Slovenia, in 1978, 1991, and 1995, respectively. Since 1988, he has been a Researcher and a Professor with the Department of Electrical Engineering, Faculty of Electrical Engineering and Computer Science, Institute for Power Systems, Maribor. His research interests include switching devices and switchgear.